Battery Performance Modeling on Maxwell X-57

Jeffrey C. Chin,* Sydney L. Schnulo,† Thomas B. Miller,‡
Kevin Prokopius,§ and Justin Gray¶
NASA Glenn Research Center, Cleveland, OH, 44135, U.S.A.

Accurate battery thermal estimation, state-of-charge (SOC), and voltage response estimates are essential for mission planning of battery powered electric aircraft. Numerous works exist that outline simulation of lithium-ion battery cells with thermal considerations, so this paper serves to expand the experimentally validated regime into higher temperatures and to Li-ion batteries in the 18650 form factor. The work compares various battery modeling methods with operational and thermal conditions unique to aircraft. The technique used to fit equivalent circuit model parameters to experimental data is also comprehensively detailed in this report, with thermal conditions matched to the X-57 aircraft configuration. Multiple comparisons between the model and various transient profiles are then summarized.

An overview of X-57 battery configuration is also provided. The voltage and state of charge response of the battery impact the performance and thermal characteristics of multiple components in the aircraft. These vehicle level impacts of the experimentally derived data are plotted against previously assumed performance maps. Lastly, access to the raw maps and experimental data is provided in the appendix.

I. Nomenclature

Ah	Ampere hours ($A * 3600 * s$)
α	thermal diffusivity ($\frac{m^2}{s}$)
C	discharge C-rate (A)
$^\circ C$	degrees Celsius ($^\circ C$)
C_{Th}	Thevenin polarization capacitance (F)
Cp	specific heat ($\frac{J}{K}$)
D	diameter (m)
ΔV	change in Voltage (V)
η_{pack}	pack efficiency
γ_a	atmospheric ratio of specific heats
I_L	line current (A)
n_p	number in parallel
n_s	number in series
P	power (kW)
Pr	Prandtl Number
Q	battery capacity (Ah)
Re	Reynolds number
R_0	internal resistance (Ω)
R_{Th}	Thevenin resistance (Ω)
SOC	state-of-charge
T	temperature (K)
U_{oc}	open circuit voltage (OCV) (V)
U_L	terminal voltage (V)

*Propulsion Systems Analysis Branch, jeffrey.c.chin@nasa.gov, AIAA Member.
†Propulsion Systems Analysis Branch, sydney.l.schnulo@nasa.gov, AIAA Member.
‡Electrochemical Systems Branch, thomas.b.miller@nasa.gov
§Aerospace Engineer, Vantage Partners LLC, Brookpark OH, kevin.prokopius@nasa.gov AIAA Member.
¶Propulsion Systems Analysis Branch, justin.s.gray@nasa.gov, AIAA Member.

II. Introduction

Modeling of lithium-ion batteries is challenging due to their multivariate non-linearity. In particular, the time dependent state-of-charge, temperature, and discharge rate all impact battery performance. Battery modeling can be categorized into three main approaches: electrochemical, mathematical, and electrical. A blend between the electrical and mathematical model is chosen in this application due to it‘s fast execution speed, and relatively accurate prediction of SOC, open-circuit voltage (OCV), temperature and terminal voltage.

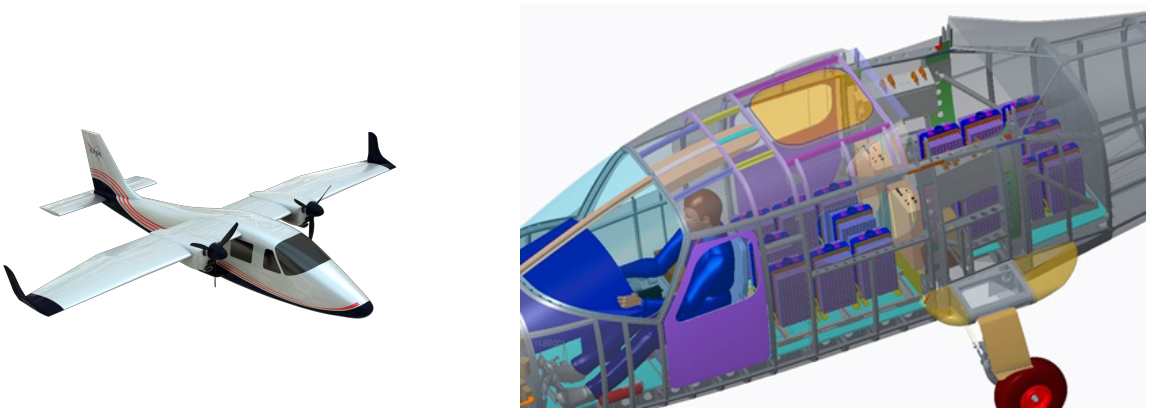

Figure 1. (Left) NASA's X-57 "Maxwell" aircraft, modification #2 variant (Right) Transparent fuselage view depicting battery location and configuration into 16 battery modules

Designing batteries in the context of an experimental aircraft is different than previous works on ground-based electric vehicles due to more stringent weight requirements. These requirements push the thermal design solution to be as minimal as possible, while maintaining safe operation against thermal runaway. An aircraft mission and power demand places a greater emphasis on capturing variations in OCV and internal resistance over capturing exact transient responses. Figure 1 shows the X-57 Mod2 vehicle design and battery placement within the fuselage.

Property	Value	Units
specific heat	0.83	J/gram-°C
cell mass	48	grams
discharge temp limits	-20 to 75	°C
max discharge rate	15	Amps
max mission discharge	9	Amps
nominal voltage	3.6	Volts
nominal capacity	3	Ah
total pack mass	350	kg
pack energy density	150	Wh/kg
vehicle weight (w/o batteries)	996	kg
min pack voltage	330	Volts
max power draw	120	kW
sub-module config	1sx20p	# of cells
module config	16sx1p	# of sub-modules
pack config	8sx2p	# of modules

Table 1. X-57 Battery Properties

Each battery module is comprised of 320 cylindrical 18650 cells developed by Samsung (SDI 18650-30Q) and contained within a solid block of aluminum with cores drilled for each individual cell. This solid pack body serves to contain a cell thermal runaway event by absorbing and spreading the heat sufficiently, with a central blow-off vent to release pressure gas and ejecta overboard in the event of a cell failure.

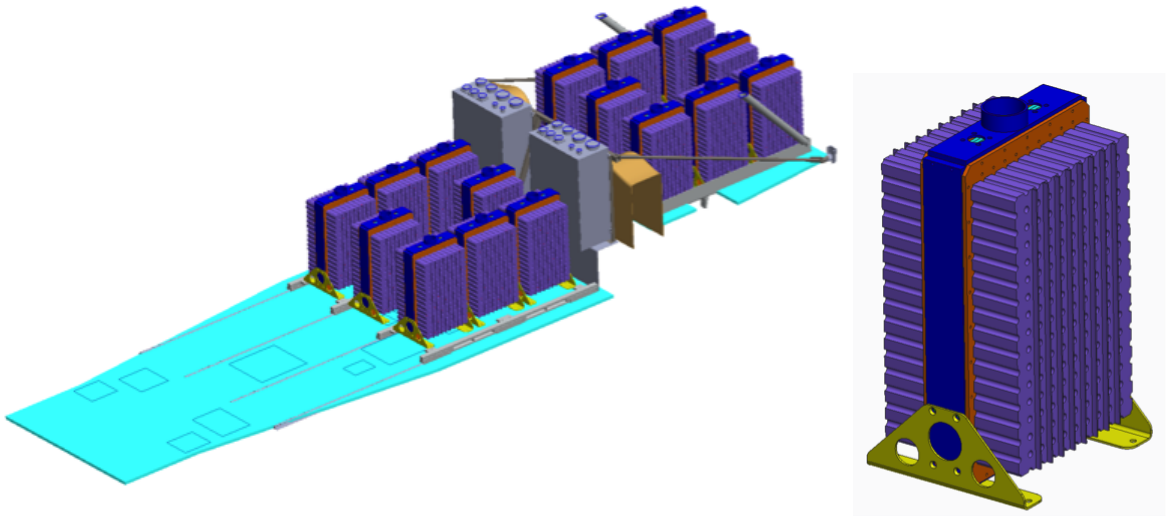

Figure 2. Isolated view of the battery pack and module

III. Battery Loss Modeling

A. Equivalent Circuit Model

In order to capture transient voltage effects, non-linear capacity and thermal effects within the battery and subsequent components, a model is required to simulate battery internal resistance and voltage as a function of current draw, SOC, and battery temperature.[1,2] Existing models for Lithium Ion batteries are explored in detail in multiple studies.[3,4] These models are comprised of equivalent circuit models of varying complexity. The single RC block Thevenin model is identified as the ideal model for this application due to its simplicity and data availability, while still being able to capture transient effects and track state-of-charge within 2% accuracy of experimental data. This model, shown in Figure 3, is composed of a voltage source, an internal resistance, and a parallel resistor-capacitor (RC) block to capture polarization effects.

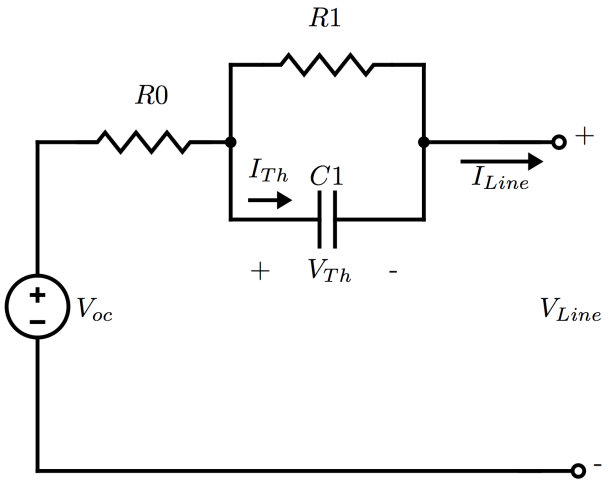

Figure 3. Thevenin equivalent circuit model of a battery containing a transient RC block.

The values of each of these circuit components are interpolated from performance maps as a function of the state-of-charge, current and temperature.

$$U_{oc}, C_{Th}, R_0, R_{Th} = f(SOC, T_{batt}) \tag{1}$$

Subscripts oc, Th and L in Figure 3 and Equation 1 refer to open circuit, Thevenin and line, respectively. The Thevenin voltage U_{Th}, battery state-of-charge SOC and battery temperature T_{batt} are treated as integrated

states over the course of the simulation, subject to the following differential equations[5] where Q_{max} is the capacity of a single cell, which is 3 Ah in our model. Each of the aircraft's two battery packs are arranged with 128 cells in series (n_{series}), and 40 in parallel ($n_{parallel}$). The line voltage is computed from the open circuit and Thevenin voltage as:

$$U_L = U_{oc} - U_{Th} - I_L R_0 \tag{2}$$

$$\frac{dU_{Th}}{dt} = \frac{I - \frac{U_{Th}}{R_{Th}}}{C_1} \tag{3}$$

$$\frac{dSOC}{dt} = -\frac{I}{3600 * Q_{max}} \tag{4}$$

Note that U_{Th} and SOC are rates to be integrated over the mission. The electric properties of the battery pack are then:

$$I_{pack} = I_L \cdot n_{parallel} \tag{5}$$

$$U_{pack} = U_L \cdot n_{series} \tag{6}$$

$$P_{pack} = (I_{pack} \cdot U_{pack})\eta_{pack} - P_{aux} \tag{7}$$

where η_{pack} is an efficiency knockdown to compensate for pack level losses and P_{aux} accounts for auxiliary power draw. The battery model is then integrated into a full aircraft model based on a demanded power driven by the overall vehicle equations of motion and propulsion models. A Newton solver is used to find the current load on a single cell (I_L) such that the power output from the battery pack is equal to the demanded power after all the efficiency knockdowns and transient responses:

$$\mathcal{R}(I_L) = P_{out-battery} - P_{pack} \tag{8}$$

The battery output power is determined by reducing the requested motor input power by the efficiency losses from the wires and inverters. Using this model, the heat output of the battery and voltage of the batteries can be accurately tracked. The battery model also dictates the current and voltage levels supplied to the other electric components, which is critical for estimating their thermal loads. The heat power generated by each cell P_{heat} can be quantified, as well as the net heat load P_{net} and cell temperature rise $\frac{dT}{dt}$:

$$P_{heat} = {I_L}^2 * (R_0 + R_{Th}) \tag{9}$$

$$P_{net} = P_{heat} - \underbrace{hA(T_{batt} - T_{amb})}_{\text{convective heat out}} \tag{10}$$

$$\frac{dT}{dt} = \frac{P_{net}}{m * C_p} \tag{11}$$

In these equations, h, m, and C_p are the heat transfer coefficient, cell mass, specific heat respectively. It's important to note that that heat capacity of the cell is impacted by the surrounding aluminum core and should be mass averaged for determining the bulk temperature rise of the entire system.

IV. Model Parameter Extraction Using Cell Characterization

A combination of battery testing and modeling are done to distill the characteristics of the lithium ion cells that make up the battery packs into a series of performance maps. Since the Thevenin equivalent circuit variable values (R_0, R_{Th}, C_{Th}, and U_{oc}) are a function of state-of-charge and temperature, a series of tests are done on individual cells at different temperatures, and the data collected in these experiments are used to extract the values of open circuit voltage source (U_{oc}), internal resistance (R_0), and the parallel RC (C_{Th}, R_{Th}) block. The model is adaptable to different cell chemistry and configurations, assuming performance data at the cell level is available.

A. Battery Cell Test Setup and Data Collection

Cell tests were performed using an Arbin BT-2000. Data was collected every 60 seconds during rest periods, and at a rate of 2 samples/second during current pulses. Total test elapsed time, step pulse time, step index, current, voltage, discharge energy, and two temperature readings were recorded with each sample.

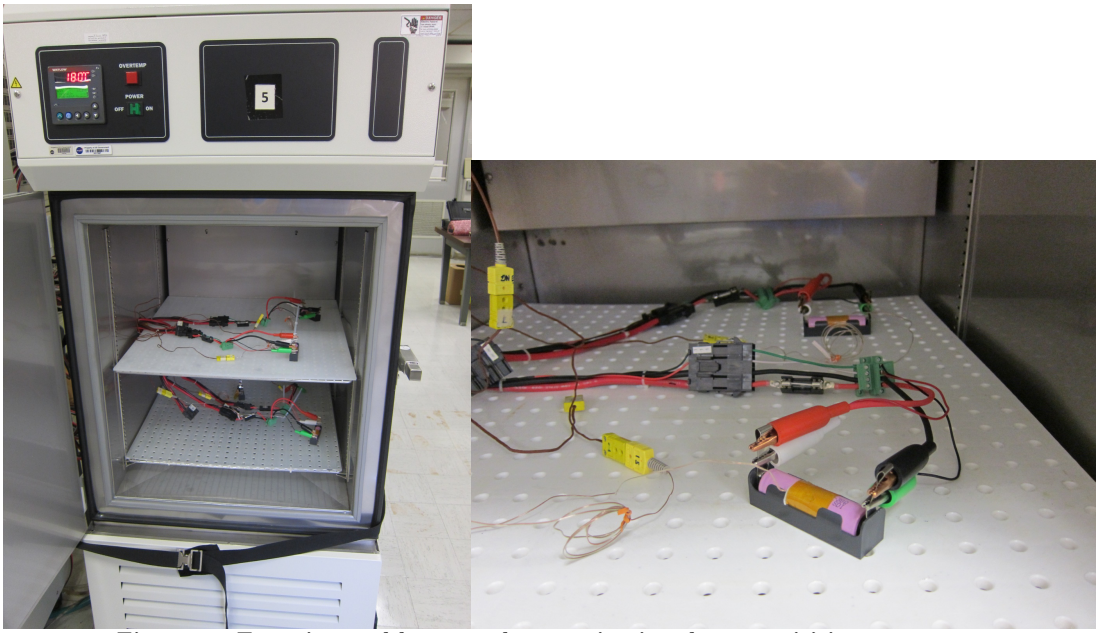

Figure 4. Experimental battery characterization data acquisition test setup.

The cells are placed in a temperature controlled chamber and outfitted with a thermocouple, as shown in Figure 4. Each temperature and discharge test combination is conducted on three lithium-ion cells. Multiple cells were tested under identical conditions to quantify variations between cells, and the 60°C test was performed on six cells, three new cells and three previously cycled cells to compare the effects of aging. Long pauses between pulses ensured the cells remained near a constant temperature. This procedure allows equivalent circuit parameters to be fit based on the pulse transients for five different temperatures and 30 different states of charge. Each of these pulses is used to compute four battery parameters to cover all the possible battery conditions it may see during flight aboard the X-57 aircraft.
Test Procedure:

1. Perform cell wake-up cycles and charge:
   - C/2 Charge @ 20°C
   - CV Taper @ 20°C to C/20 (0.15A)
2. Turn on temperature chamber and allow air and cells to stabilize to the specified chamber temperature for two hours. Start data acquisition.
3. Begin discharging cells at the rates specified in the test matrix for a pulse duration of two minutes.
4. Allow cells to return to specified chamber temperature for 20 minutes.

5. If the temperature sensor shows that cell temperature increases more than 2 degrees, terminate the test.

6. Repeat steps 3-5 until batteries are discharged to three volts.

7. C/2 charge to 20% SOC (0.6Ah) to stabilize cells.

8. Remove cycled cells and repeat with three fresh cells at the next temperature step in the test matrix.

Test Number	Temperature	Cell Discharge Rates	Cells per test
1	0°C	0.8C, 1C, 2C	3
2	20°C	0.8C, 1C, 2C	3
3	30°C	0.8C, 1C, 2C	3
4	45°C	0.8C, 1C, 2C	3
5	60°C	1C	6

Table 2. Test Matrix

V. Parameter Extraction

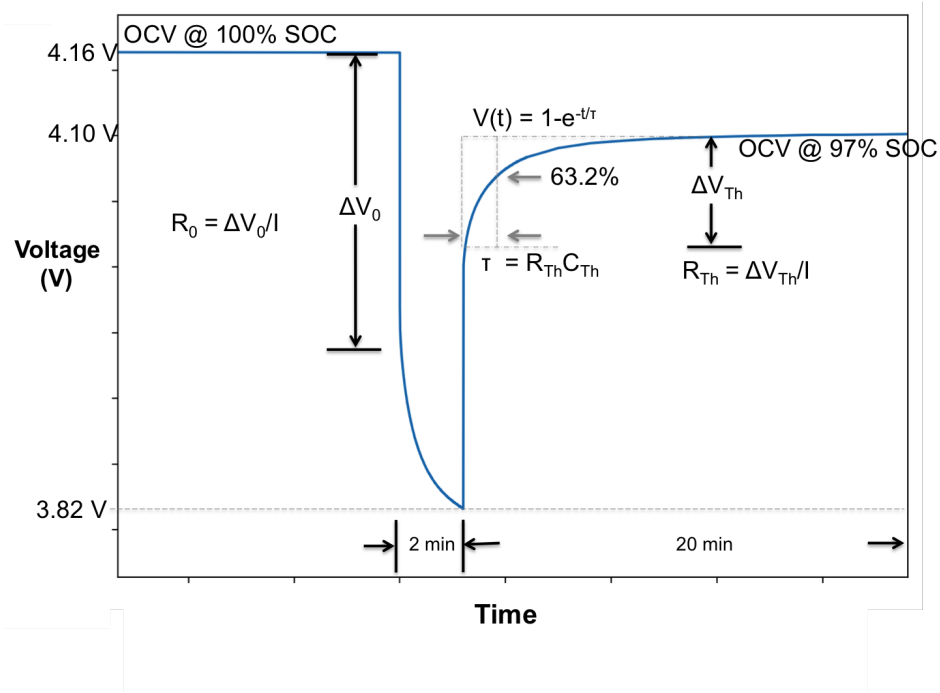

Figure 5. Characterization from current pulse

In Figure 5 a sample voltage response is shown with annotations showing how each circuit characteristic is derived. Before each pulse, the voltage is steady at the OCV point corresponding to the SOC. During the current pulse, the voltage drops rapidly by a distance ΔV_0 corresponding to the product of $R_0 * I$. The subsequent logarithmic transient is then defined by the Thevenin resistance and capacitance. The non-linear return to the next OCV has a time constant equal to $R_{Th} * C_{Th}$, which is equal in magnitude to the time in seconds it takes to return 63.2% or $(1 - \frac{1}{e})$ of ΔV_{Th}. This parameter extraction is repeated for every pulse corresponding to a different SOC.

A. Modeling Approach to Parameter Extraction

After the series of battery tests, the collected battery discharge data can be input into a model which uses a least squared optimization to characterize the cells, matching computes values to measured values. The experimental current discharge curve for each temperature are input into the parameter extraction

model. Internal resistance (R_0), Thevenin resistance (R_{Th}), Thevenin capacitance (C_{Th}), and open circuit voltage (U_{oc}) are varied using a solver until the model computed voltage and the experimental voltage data match. The model computes each variable across the state-of-charge profile until the least squared regression minimizing the difference between experimental and computed voltages are satisfied. This computation yields a series of lookup tables which allow the battery model to interpolate R_0, R_{Th}, C_{Th}, and U_{oc} as a function of battery state-of-charge and temperature.

By separating the data into individual pulses, this process can be reduced to a linear algebra least squares problem as written:

$$x = \begin{bmatrix} SOC \\ U_{Th} \\ U_{Th} \end{bmatrix}$$

$$\dot{x} = Ax + bu = \begin{bmatrix} SOC \\ U_1 \\ U_2 \end{bmatrix} = \begin{bmatrix} 0 & 0 & 0 \\ 0 & \frac{-1}{R_1 C_1} & 0 \\ 0 & 0 & \frac{-1}{R_2 C_2} \end{bmatrix} \begin{bmatrix} SOC \\ U_1 \\ U_2 \end{bmatrix} + \begin{bmatrix} \frac{-1}{\alpha} \\ \frac{1}{C_1} \\ \frac{1}{C_2} \end{bmatrix} \tag{12}$$

$$y = Cx + Du = \begin{bmatrix} \alpha & -1 & -1 \end{bmatrix} \begin{bmatrix} SOC \\ U_1 \\ U_2 \end{bmatrix} + \begin{bmatrix} -R_s \end{bmatrix} I$$

$$\tau = R_{Th} C_{Th} \tag{13}$$

$$V_1(t_{charge}) = R_1 * I_0 * (1 - e^{\frac{-t}{\tau}}) \tag{14}$$

$$V_1(t_{discharge}) = R_1 * I_0 * (1 - e^{\frac{-a}{\tau}}) e^{\frac{t-a}{\tau}} \tag{15}$$

$$\underbrace{\begin{bmatrix} y[k+1] \\ y[k+2] \\ \vdots \\ y[k+m] \end{bmatrix}}_{\text{b}} = \underbrace{\begin{bmatrix} y[k] & I[k] & I[k+1] \\ y[k+1] & I[k+1] & I[k+1] \\ \vdots & \vdots & \vdots \\ y[k+m-1] & ... & I[k+m] \end{bmatrix}}_{\text{A}} \underbrace{\begin{bmatrix} \alpha_0 \\ b_1 \\ b_2 \end{bmatrix}}_{\text{x}}$$

$$A \backslash b = x \tag{16}$$

Depending on the current draw and temperature, the duration of each experiment is variable. Maps are calculated by creating n breakpoints to match n pulses, equally spaced from 1 to the lowest SOC. In post-processing, all maps are re-interpolated to a consistent number of breakpoints from 0 to 1. This allows a single dense 2-dimensional table to be created across a range of temperatures and charge levels.

B. Results

By creating an electrical model to mimic the cell response, it is designed to handle any arbitrary discharge current. Therefore as expected, the model performed equally well at different discharge rates. This is shown in Figure 6, where the voltage response of two sets of experimental data and model fits are overlaid. Despite the voltages diverging between different discharge rates, the same model performed equally well on both. As a check for cell manufacturing consistency, it was also found that there was insignificant difference between

cell performance exposed to the same testing conditions. Variation between temperatures is largely due to resistance. Figure 7 shows experimental data for comparing cell behavior across five temperatures. The capacitance and voltage parameters did not change significantly between temperature and discharge rate tests beyond 20 °C.

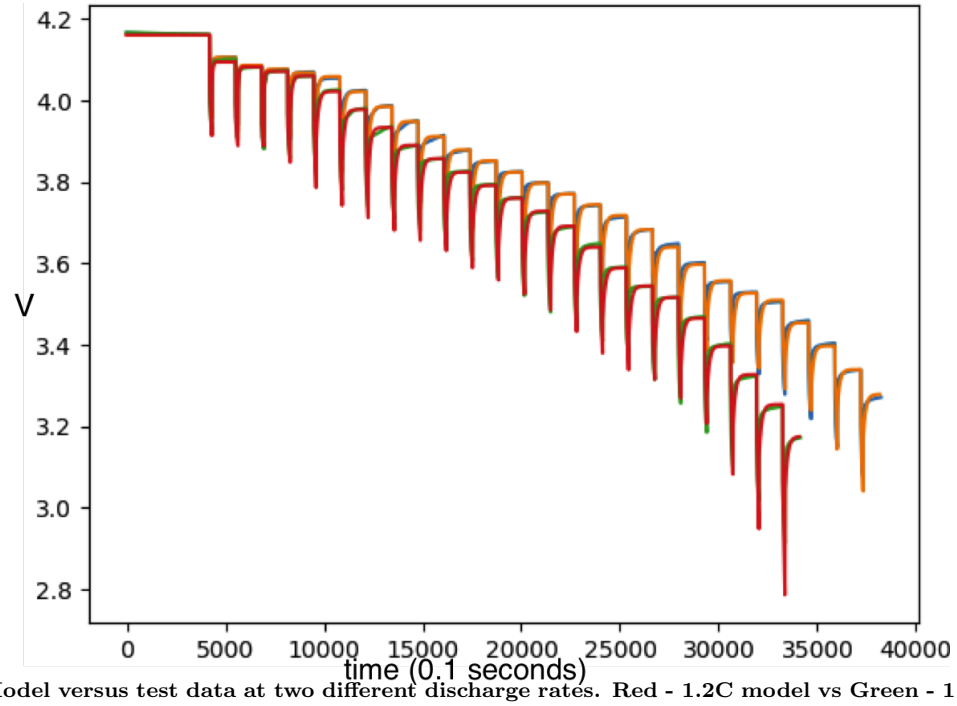

Figure 6. Model versus test data at two different discharge rates. Red - 1.2C model vs Green - 1.2C test data, Orange 1C model vs Blue 1C test data, shows the same model working regardless of discharge rate.

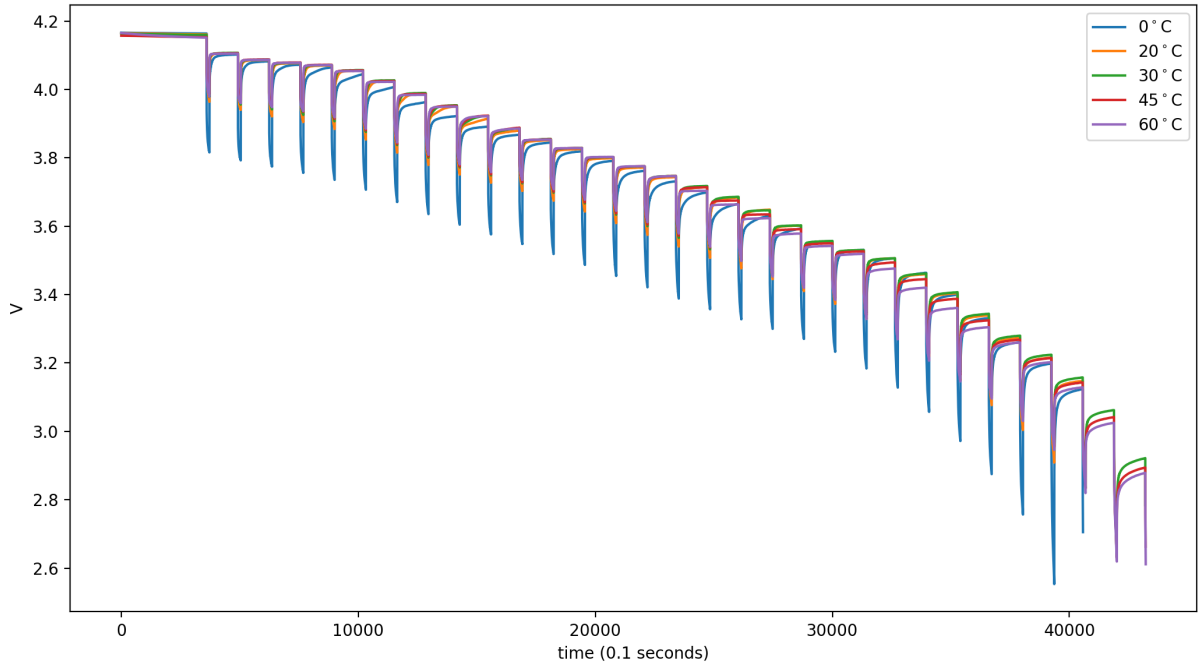

Figure 7. Battery voltage response to current pulses across five temperatures

Figure 8 shows the variation of each parameter across 4 temperatures and a series of SOCs. Capacitance is not shown, since it wasn't shown to have significant variant across temperature or charge. This parameter can stay at a value of 2000. The open-circuit voltage decreases with reduced SOC, and it should be noted that this curve is not expected to match battery manufacturer performance curves. These curves are reproduced

with the model in Figure 9. Thevenin resistance follows a slow upward trend with decreasing charge, with a noticeable jump in resistance for colder temperatures. R_0 also increases substantially at 0°C, but remains flat until very low SOC.

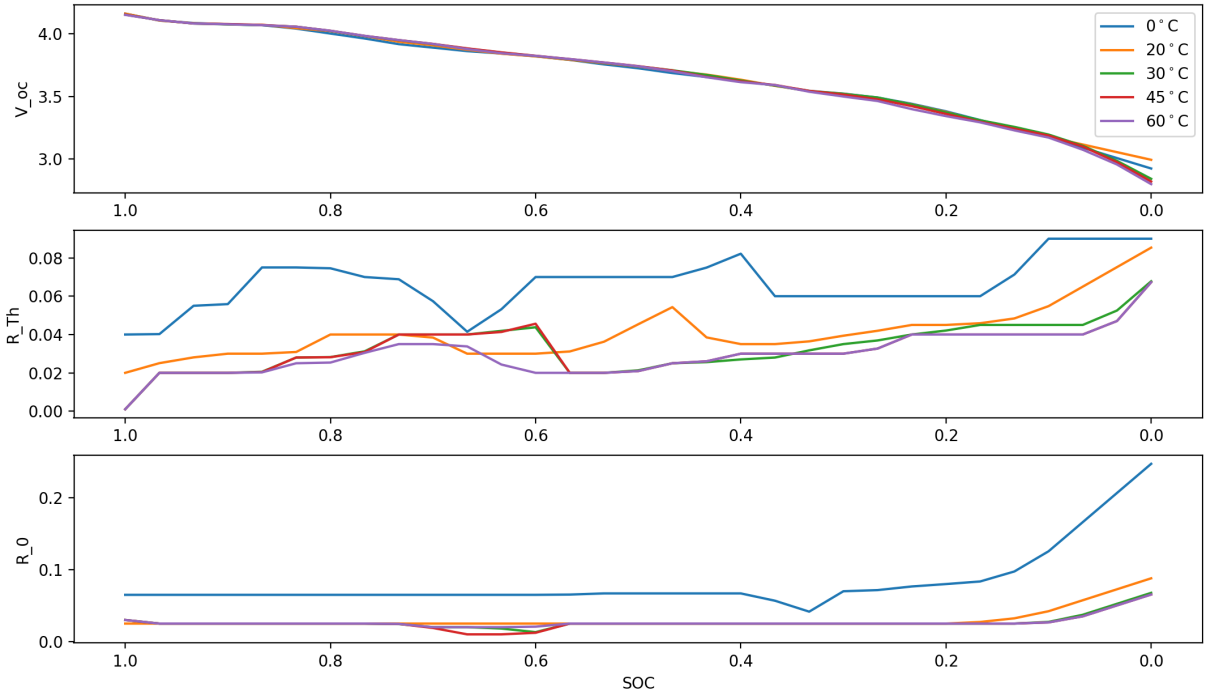

Figure 8. Parameter variation with temperature and SOC

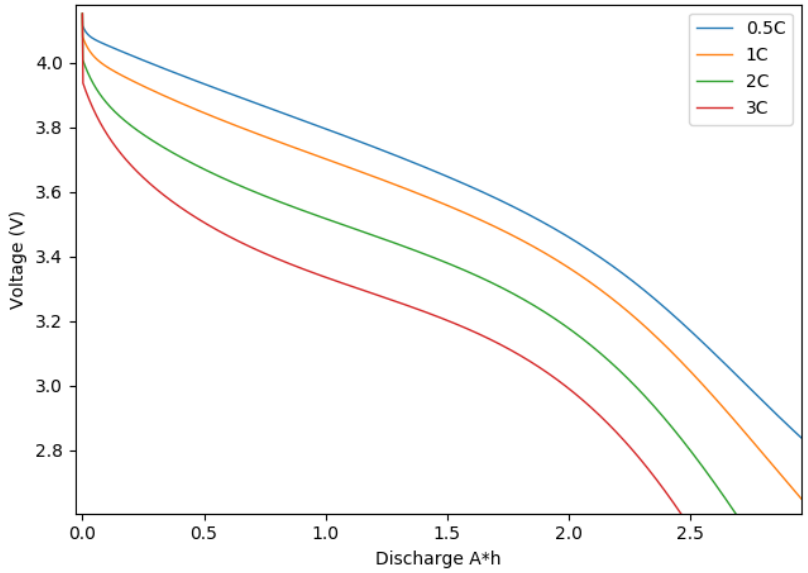

Figure 9. Replication of standard manufacturer performance curve

Figure 9 shows the battery model used to simulate a standard cell manufacturer performance curve over a steady discharge rate. Shown in Figure 10 is the battery response to a nominal flight profile compared to the model. The top graph shows test voltage data in blue, and the prediction model in orange. The bottom graph shows the same profile but shows predicted temperature. A green line is also plotted to show temperature estimates assuming a constant loss rate of 8 percent. As expected, assuming a constant

efficiency over-estimates the initial losses at high states of charge and under-estimates the losses at low states of charge. This highlights the benefit of the model in capturing non-linear resistances to accurately track temperature.

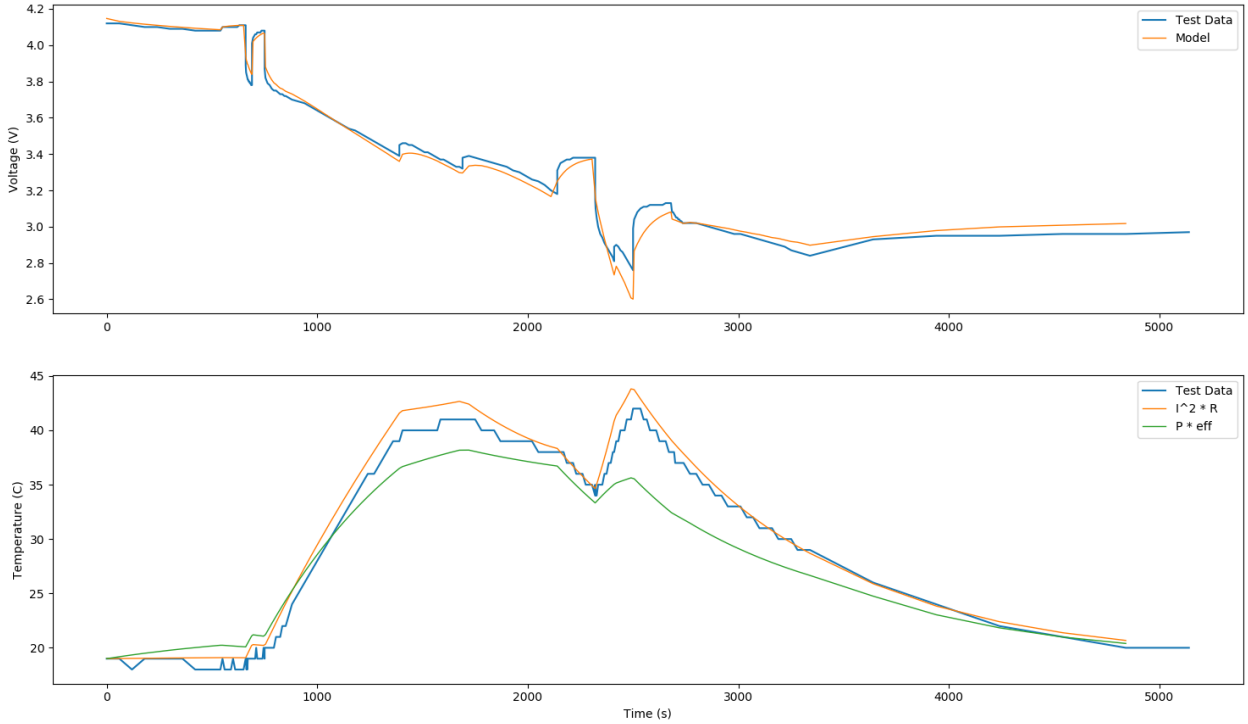

Figure 10. Model performance against a nominal flight profile

Applying these new battery characteristics to a full vehicle model of X-57 resulted in a decrease in expected vehicle performance over the previously assumed prismatic cell data. The notional mission profile shown below depicts the reduction in cruise time of the vehicle.

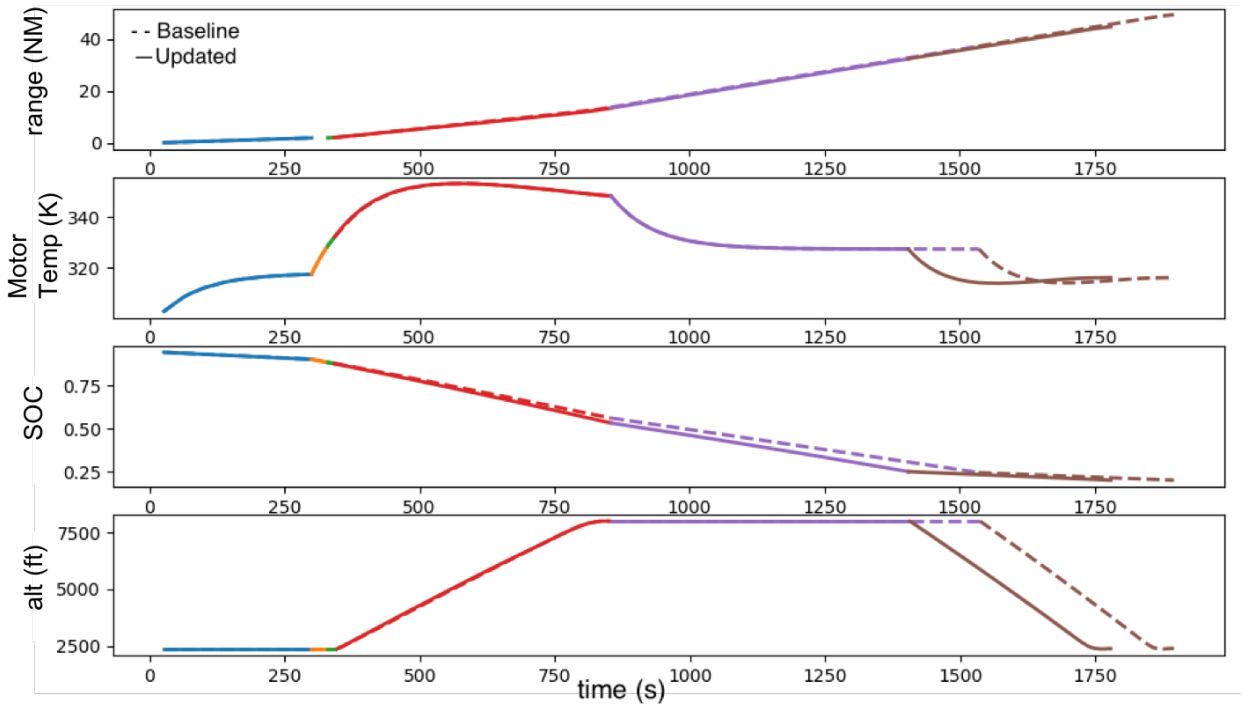

Figure 11. Impact in performance at the vehicle level, compared to baseline maps. Each color represents a different mission segment. Taxi, motor check, climb, cruise, and descent respectively from left to right.

VI. Model Limitations

The model does not currently account for capacity fade and aging due to high discharge rates or repeated cycles. Modifiers could be added to the model,[6] however it was deemed unnecessary for X-57 which will only be flown a very limited number of times. Given the limited test points, the model is not well fit to experimental data at states of charge below 20 percent where the behavior becomes more divergent. This limitation is deemed acceptable given that the vehicle must avoid fully draining the battery to avoid permanent capacity fade. As discussed in section III, there are numerous higher fidelity battery modeling techniques, and this method was chosen for its simplicity and speed.

VII. Conclusions and Future Work

Various figures of merit were used to compare a purely mathematical battery modeling method to a combined electrical and analytical model. The parameters necessary for the equivalent circuit model were experimentally derived using the described test procedures and optimization routine. The error in each type of model was quantified for a range of transient profiles and operating temperatures. The purely analytical model provides a more generic tool set, that can be more readily defined using manufacturer's specification data. The electrical model is able to capture a higher degree of transient behavior over a range of charge levels, which becomes increasingly critical for transients involving many throttle changes. Both methods can be used interchangeably as the basis for pack level calculations and vehicle level models, depending on the designer's needs.

VIII. Acknowledgements

The authors would like to thank the rest of the X-57 team, the battery team, and the Electric Power Systems for their collaboration. Additional thanks to the NASA Flight Demonstration and Capabilities Project for sponsoring this work.

References

[1]Hu, Y., Yurkovich, S., Guezennec, Y., and Yurkovich, B., "Electro-thermal battery model identification for automotive applications," *Journal of Power Sources*, pp 449-457, Journal of Power Sources, 2010.

[2]Abbas, F., Daniel J., A., Karsten, P., and Stefano, L., "A Study on Battery Model Parameterisation Problem Application-Oriented Trade-offs between Accuracy and Simplicity," *International Federation of Automatic Control*, pp 48-53, Elsevier, 2016.

[3]Huria, T., Ceraolo, M., Gazzarri, J., and Jackey, R., "High Fidelity Electrical Model with Thermal Dependence for Characterization and Simulation of High Power Lithium Battery Cells," *Electric Vehicle Conference (IEVC)*, pp 1-8, IEEE International, March 2012.

[4]Xiaosong, H., Shengbo, L., and Huei, P., "A comparative study of equivalent circuit models for Li-ion batteries," *Journal of Power Sources*, pp 359-367, Journal of Power Sources, 2012.

[5]He, H., Rui, X., and Jinxin, F., "Evaluation of lithium-ion battery equivalent circuit models for state of charge estimation by an experimental approach," *Electric Vehicle Conference (IEVC)*, 4.4 582-598, Energies, March 2011.

[6]Ning, G., Haran, B., and Popov, B. N., "Capacity fade study of lithium-ion batteries cycled at high discharge rates," *Journal of Power Sources*, pp 160-169, Journal of Power Sources, 2002.

The raw data can be found at:
https://github.com/jcchin/Battery-Performance-Modeling-on-Maxwell-X_57/blob/master/Data.zip

The code repository can be found at:
https://github.com/jcchin/Battery-Performance-Modeling-on-Maxwell-X_57/tree/master/code

A. Battery Performance Maps

```
battery.T_bp = np.array([0., 20., 30., 45.])
battery.SOC_bp = np.array( [0.        , 0.03333333, 0.06666667, 0.1       , 0.13333333, 0.16666667,
 0.2       , 0.23333333, 0.26666667, 0.3       , 0.33333333, 0.36666667,
 0.4       , 0.43333333, 0.46666667, 0.5       , 0.53333333, 0.56666667,
 0.6       , 0.63333333, 0.66666667, 0.7       , 0.73333333, 0.76666667,
 0.8       , 0.83333333, 0.86666667, 0.9       , 0.93333333, 0.96666667,
 1.        ] )
battery.tU_oc = np.array([ [2.92334783,3.00653623,3.08972464,3.17291304,3.23989855,3.31010145,
 3.3803913 ,3.44033333,3.49033333,3.52169565,3.54391304,3.58695652,
 3.62095652,3.65437681,3.68604348,3.72430435,3.75531884,3.79102899,
 3.82030435,3.84181159,3.86124638,3.88921739,3.91686957,3.96223188,
 4.00169565,4.04117391,4.06849275,4.07573913,4.08571014,4.10571014,
 4.161     ] ,  [2.99293893,3.05400763,3.11507634,3.17614504,3.23506616,3.30371247,
 3.37521374,3.43605852,3.48697455,3.5200229 ,3.54251908,3.58374046,
 3.6329313 ,3.67379644,3.70287532,3.73784733,3.76526463,3.79174809,
 3.81922901,3.84108142,3.87212214,3.90738931,3.93615267,3.98113995,
 4.02093893,4.04504071,4.07114758,4.07583969,4.08371501,4.10560814,
 4.161     ] ,  [2.84084639,2.98428484,3.1050295 ,3.19464496,3.25566531,3.309059  ,
 3.37185148,3.43473652,3.49059613,3.51955239,3.541353  ,3.58558494,
 3.62641607,3.6708881 ,3.70814547,3.7392177 ,3.76822075,3.79592981,
 3.82260427,3.84986368,3.88146592,3.91739674,3.94798779,3.98188403,
 4.02274568,4.05623296,4.06830824,4.07468871,4.08175788,4.10853306,
 4.153     ] ,  [2.81925101,2.97410931,3.09861134,3.18674899,3.24142105,3.29678138,
 3.35963563,3.42195951,3.47637247,3.51383806,3.54319838,3.59076923,
 3.61940891,3.65574089,3.7067004 ,3.74153441,3.77023887,3.79773684,
 3.82421053,3.85139271,3.88311336,3.91906478,3.94918219,3.98310931,
 4.02401215,4.05611741,4.07036842,4.07774494,4.08190283,4.10867206,
 4.153     ] ])
battery.tC_Th = np.array([ [2000.,2000.,2000.,2000.,2000.,2000.,2000.,2000.,2000.,2000.,2000.,2000.,
 2000.,2000.,2000.,2000.,2000.,2000.,2000.,2000.,2000.,2000.,2000.,2000.,
 2000.,2000.,2000.,2000.,2000.,2000.,2000.] ,  [2000.,2000.,2000.,2000.,2000.,2000.,2000.,2000.,2000.,2000.,2000.,2000.,
 2000.,2000.,2000.,2000.,2000.,2000.,2000.,2000.,2000.,2000.,2000.,2000.,
 2000.,2000.,2000.,2000.,2000.,2000.,2000.] ,  [2000.,2000.,2000.,2000.,2000.,2000.,2000.,2000.,2000.,2000.,2000.,2000.,
 2000.,2000.,2000.,2000.,2000.,2000.,2000.,2000.,2000.,2000.,2000.,2000.,
 2000.,2000.,2000.,2000.,2000.,2000.,2000.] ,  [2000.,2000.,2000.,2000.,2000.,2000.,2000.,2000.,2000.,2000.,2000.,2000.,
 2000.,2000.,2000.,2000.,2000.,2000.,2000.,2000.,2000.,2000.,2000.,2000.,
 2000.,2000.,2000.,2000.,2000.,2000.,2000.] ])
battery.tR_Th = np.array([ [0.09      ,0.09      ,0.09      ,0.09      ,0.07130435,0.06      ,
 0.06      ,0.06      ,0.06      ,0.06      ,0.06      ,0.06      ,
 0.08217391,0.07492754,0.07      ,0.07      ,0.07      ,0.07      ,
 0.07      ,0.05318841,0.04144928,0.0573913 ,0.06884058,0.07      ,
 0.07456522,0.075     ,0.075     ,0.05586957,0.055     ,0.04021739,
 0.04      ] ,  [0.08534351,0.07516539,0.06498728,0.05480916,0.04838931,0.04589059,
 0.045     ,0.045     ,0.04195929,0.03937405,0.03642494,0.035     ,
 0.035     ,0.03848601,0.05430025,0.04534351,0.03624682,0.03115776,
 0.03      ,0.03      ,0.03      ,0.03839695,0.04      ,0.04      ,
 0.04      ,0.03089059,0.03      ,0.03      ,0.02807125,0.02505344,
 0.02      ] ,  [0.0677823 ,0.05252289,0.045     ,0.045     ,0.045     ,0.045     ,
 0.04207528,0.04      ,0.03690234,0.035     ,0.0317294 ,0.02798576,
 0.027     ,0.025588  ,0.025     ,0.02129705,0.02      ,0.02      ,
 0.04377416,0.04190234,0.04      ,0.04      ,0.04      ,0.03121058,
 0.02820753,0.028     ,0.02055341,0.02      ,0.02      ,0.02      ,
 0.001     ] ,  [0.06728745,0.04704453,0.04      ,0.04      ,0.04      ,0.04      ,
 0.04      ,0.04      ,0.03267206,0.03      ,0.03      ,0.03      ,
 0.03      ,0.02603239,0.025     ,0.02091093,0.02      ,0.02      ,
 0.04562753,0.04133603,0.04      ,0.04      ,0.04      ,0.0308502 ,
 0.02814575,0.028     ,0.02038866,0.02      ,0.02      ,0.02      ,
 0.001     ] ])
battery.tR_0 = np.array([ [0.2473913 ,0.20681159,0.16623188,0.12565217,0.09753623,0.08362319,
 0.08      ,0.07666667,0.0715942 ,0.07      ,0.0415942 ,0.05681159,
 0.067     ,0.067     ,0.067     ,0.067     ,0.067     ,0.06537681,
 0.065     ,0.065     ,0.065     ,0.065     ,0.065     ,0.065     ,
 0.065     ,0.065     ,0.065     ,0.065     ,0.065     ,0.065     ,
 0.065     ] ,  [0.08801527,0.07274809,0.05748092,0.04221374,0.03231552,0.02722646,
 0.025     ,0.025     ,0.025     ,0.025     ,0.025     ,0.025     ,
 0.025     ,0.025     ,0.025     ,0.025     ,0.025     ,0.025     ,
 0.025     ,0.025     ,0.025     ,0.025     ,0.025     ,0.025     ,
 0.025     ,0.025     ,0.025     ,0.025     ,0.025     ,0.025     ,
 0.025     ] ,  [0.0677823 ,0.05252289,0.03726348,0.02733469,0.025     ,0.025     ,
 0.025     ,0.025     ,0.025     ,0.025     ,0.025     ,0.025     ,
 0.025     ,0.025     ,0.025     ,0.025     ,0.025     ,0.025     ,
 0.01311292,0.01809766,0.02      ,0.02      ,0.02430824,0.025     ,
 0.025     ,0.025     ,0.025     ,0.025     ,0.025     ,0.025     ,
 0.03      ] ,  [0.06546559,0.0502834 ,0.03510121,0.02663968,0.025     ,0.025     ,
 0.025     ,0.025     ,0.025     ,0.025     ,0.025     ,0.025     ,
 0.025     ,0.025     ,0.025     ,0.025     ,0.025     ,0.025     ,
 0.01218623,0.01      ,0.01      ,0.01890688,0.02451417,0.025     ,
 0.025     ,0.025     ,0.025     ,0.025     ,0.025     ,0.025     ,
 0.03      ] ])
```

Test Number	Cell S/N	Chamber Temp. (^{o}C)	Cell Discharge Rate	Cell Discharge Rate	Cell Discharge Rate	Cell Discharge Rate
1	027, 028, 029	20	1C	1.2C	0.8C	3C
2	030, 031, 032	0	1C	1.2C	0.8C	3C
3	033, 034, 035	10	1C	1.2C	0.8C	3C
4	036, 037, 039	40	1C	1.2C	0.8C	3C
5	040, 041, 042	30	1C	1.2C	0.8C	3C
6	043, 044, 045	45	1C	1.2C	0.8C	3C
7	047, 048, 049, 027, 028, 029	60	1C	-	-	-

Figure 12. Test Matrix

Test Date	Lot #	Cell S/N	Chamber Temp. @ Discharge (°C)	Discharge Rate	Cycle Index	Discharge Capacity (Ah)	Discharge Energy (Wh)	Discharge Time (s)	Notes
4/24/2018 - 4/25/2018	1	027	20	1C	30	2.941	10.393	3590.38	Chamber #6 (Controller SP @ 20°C Charge, 20°C Discharge)
		028			30	2.939	10.387	3579.80	
		029			30	2.932	10.353	3583.74	
		030	0	1C	29	2.788	9.569	3395.74	Chamber #5 (Controller SP @ 18°C Charge, -2°C Discharge)
		031			29	2.793	9.659	3405.28	
		032			29	2.788	9.609	3396.33	
4/25/18	1	027	20	1.2C	25	2.923	10.260	2973.00	Chamber #6 (Controller SP @ 20°C Charge, 20°C Discharge)
		028			25	2.921	10.258	2966.72	
		029			25	2.914	10.231	2966.38	
		030	0	1.2C	24	2.753	9.329	2795.74	Chamber #5 (Controller SP @ 18°C Charge, -2°C Discharge)
		031			24	2.761	9.454	2804.90	
		032			24	2.755	9.402	2798.03	
4/26/2018 - 4/27/2018	1	027	20	0.8C	38	2.955	10.516	4508.01	Chamber #6 (Controller SP @ 20°C Charge, 20°C Discharge)
		028			38	2.952	10.504	4501.33	
		029			38	2.943	10.470	4500.66	
		030	0	0.8C	36	2.805	9.756	4267.66	Chamber #5 (Controller SP @ 18°C Charge, -2°C Discharge)
		031			36	2.811	9.834	4286.66	
		032			36	2.807	9.814	4272.49	
4/27/18	1	027	20	3C	10	2.803	9.329	1140.27	Chamber #6 (Controller SP @ 20°C Charge, 20°C Discharge)
		028			10	2.795	9.301	1136.48	
		029			10	2.784	9.250	1133.09	
		030	0	3C	9	2.470	7.709	1003.87	Chamber #5 (Controller SP @ 18°C Charge, -2°C Discharge)
		031			9	2.511	7.990	1020.68	
		032			9	2.492	7.906	1013.06	

Figure 13. Test 1 Summary

Test Date	Lot #	Cell S/N	Chamber Temp. @ Discharge (°C)	Discharge Rate	Cycle Index	Discharge Capacity (Ah)	Discharge Energy (Wh)	Discharge Time (s)	Notes
4/30/2018 - 5/1/2018	1	033	10	1C	30	2.898	10.192	3537.81	Chamber #6 (Controller SP @ 20°C Charge, 10°C Discharge)
		034			30	2.884	10.142	3513.15	
		035			30	2.885	10.097	3526.39	
		036	40	1C	31	2.992	10.533	3643.98	Chamber #5 (Controller SP @ 18°C Charge, 38°C Discharge)
		037			31	2.998	10.634	3655.42	
		039			31	3.000	10.637	3653.89	
5/1/18	1	033	10	1.2C	25	2.877	10.039	2926.16	Chamber #6 (Controller SP @ 20°C Charge, 10°C Discharge)
		034			25	2.868	10.022	2912.86	
		035			25	2.865	9.942	2916.32	
		036	40	1.2C	26	2.978	10.429	3024.54	Chamber #5 (Controller SP @ 18°C Charge, 38°C Discharge)
		037			26	2.982	10.513	3028.88	
		039			26	2.985	10.531	3030.94	
5/2/2018 - 5/3/2018	1	033	10	0.8C	38	2.928	10.360	4469.35	Chamber #6 (Controller SP @ 20°C Charge, 10°C Discharge)
		034			37	2.898	10.287	4419.63	
		035			37	2.899	10.239	4432.84	
		036	40	0.8C	38	2.992	10.630	4553.51	Chamber #5 (Controller SP @ 18°C Charge, 38°C Discharge)
		037			39	3.006	10.709	4584.69	
		039			39	3.012	10.744	4583.96	
5/3/18	1	033	10	3C	10	2.726	8.950	1108.79	Chamber #6 (Controller SP @ 20°C Charge, 10°C Discharge)
		034			10	2.714	8.940	1103.58	
		035			10	2.706	8.802	1101.27	
		036	40	3C	10	2.854	9.450	1159.70	Chamber #5 (Controller SP @ 18°C Charge, 38°C Discharge)
		037			10	2.875	9.613	1168.55	
		039			10	2.880	9.681	1170.66	

Figure 14. Test 2 Summary

Test Date	Lot #	Cell S/N	Chamber Temp. @ Discharge (°C)	Discharge Rate	Cycle Index	Discharge Capacity (Ah)	Discharge Energy (Wh)	Discharge Time (s)	Notes
5/4/2018 - 5/5/2018	1	040	30	1C	31	2.987	10.579	3647.17	Chamber #6 (Controller SP @ 20°C Charge, 30°C Discharge)
		041			31	2.981	10.499	3630.89	
		042			31	2.980	10.523	3642.17	
		043	45	1C	31	2.994	10.595	3646.98	Chamber #5 (Controller SP @ 18°C Charge, 44°C Discharge)
		044			31	3.006	10.625	3665.51	
		045			31	3.000	10.629	3654.30	
5/7/2018 - 5/8/2018	1	040	30	1.2C	26	2.975	10.470	3026.36	Chamber #6 (Controller SP @ 20°C Charge, 30°C Discharge)
		041			26	2.972	10.406	3018.22	
		042			26	2.969	10.404	3021.96	
		043	45	1.2C	26	2.980	10.462	3026.36	Chamber #5 (Controller SP @ 18°C Charge, 44°C Discharge)
		044			26	2.987	10.496	3034.47	
		045			26	2.987	10.570	3033.94	
5/8/2018 - 5/9/2018	1	040	30	0.8C	39	3.003	10.689	4582.68	Chamber #6 (Controller SP @ 20°C Charge, 30°C Discharge)
		041			38	2.979	10.592	4543.69	
		042			38	2.979	10.584	4555.45	
		043	45	0.8C	38	2.993	10.675	4554.37	Chamber #5 (Controller SP @ 18°C Charge, 44°C Discharge)
		044			39	3.010	10.700	4589.77	
		045			39	3.011	10.750	4582.90	
5/9/18	1	040	30	3C	10	2.864	9.570	1164.94	Chamber #6 (Controller SP @ 20°C Charge, 30°C Discharge)
		041			10	2.834	9.409	1152.41	
		042			10	2.833	9.357	1152.83	
		043	45	3C	Incomplete tests: All 3 cells went unsafe as the cell temperature safety limit of 50°C was attained during test.				Chamber #5 (Controller SP @ 18°C Charge, 44°C Discharge)
		044							
		045							
5/10/18	1	043	45	3C	10	2.879	9.694	1169.90	Chamber #5 (Controller SP @ 18°C Charge, 44°C Discharge)
		044			10	2.870	9.513	1166.66	
		045			10	2.885	9.745	1172.69	

Figure 15. Test 3 Summary

Test Date	Lot #	Cell S/N	Chamber Temp. @ Discharge (°C)	Discharge Rate	Cycle Index	Discharge Capacity (Ah)	Discharge Energy (Wh)	Discharge Time (s)	Notes
10/11/2018 - 10/12/2018	1	047	60	1C	31	2.987	10.537	3645.25	Chamber #6 (Controller SP @ 20°C Charge, 61°C Discharge)
		048			31	2.988	10.562	3645.82	
		049			31	2.989	10.562	3653.91	
		027	60	1C	31	2.972	10.528	3628.22	Chamber #5 (Controller SP @ 18°C Charge, 60°C Discharge)
		028			31	2.973	10.425	3629.36	
		029			31	2.975	10.513	3630.54	

Figure 16. Test 4 Summary

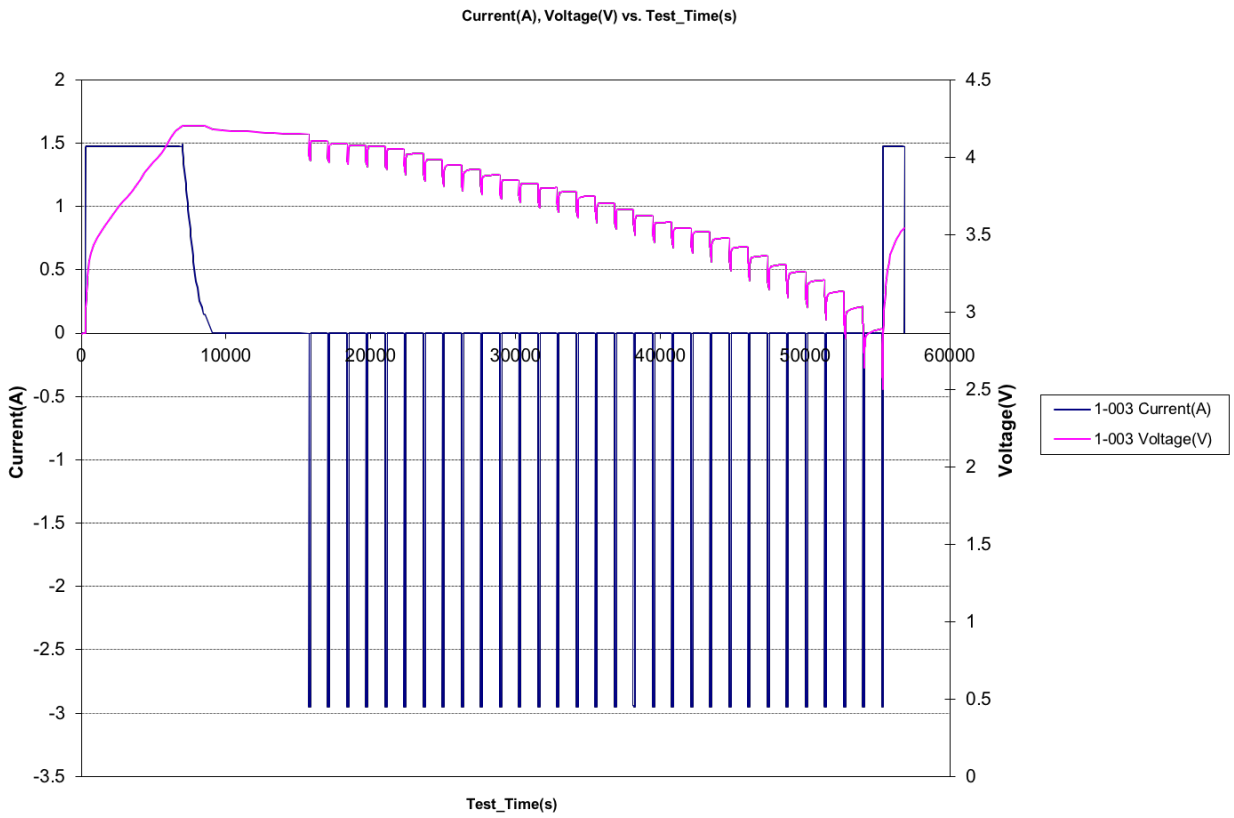

Figure 17. Test 4 Summary